

Block removal for large language models through constrained binary optimization

David Jansen¹ Roman Rausch¹ David Montero¹ Román Orús^{1,2,3}

Abstract

Compressing resource-intensive large language models by removing whole transformer blocks is a seemingly simple idea, but identifying which blocks to remove constitutes an exponentially difficult combinatorial problem. In this paper, we formulate block removal as a constrained binary optimization problem that can be mapped to a physical system (Ising model), whose energies are a strong proxy for downstream model performance. This formulation enables an efficient ranking of a large number of candidate block-removal configurations and yields many high-quality, non-trivial solutions beyond consecutive regions. We demonstrate that our approach outperforms state-of-the-art block-removal methods across several benchmarks, with performance gains persisting after short retraining, and reaching improvements of up to 6 points on the MMLU benchmark. Our method requires only forward and backward passes for a few active parameters, together with an (at least approximate) Ising solver, and can be readily applied to any architecture. We illustrate this generality on the recent NVIDIA-Nemotron-3-Nano-30B-A3B-FP8 model, which exhibits a highly inhomogeneous and challenging block structure.

1. Introduction

Large language models (LLMs) have been one of the most disruptive technological advances of this decade, demonstrating impressive capabilities in writing, summarization, and problem-solving (OpenAI, 2023). Built primarily on

¹Multiverse Computing, Parque Científico y Tecnológico de Gipuzkoa, Paseo de Miramón, 170, 20014 Donostia/San Sebastián, Spain ²Donostia International Physics Center, Paseo Manuel de Lardizabal 4, E-20018 San Sebastián, Spain ³Ikerbasque Foundation for Science, Maria Diaz de Haro 3, E-48013 Bilbao, Spain. Correspondence to: David Jansen <david.jansen@multiversecomputing.com>.

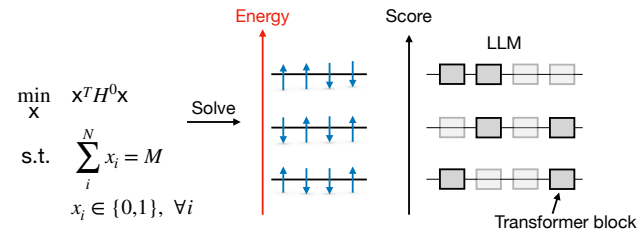


Figure 1. Sketch of our method. We formulate block pruning as a constrained binary optimization problem that can be mapped to an Ising model with fixed magnetization. Each feasible solution specifies which M out of N blocks are removed from the LLM. The optimization is constructed such that low-energy solutions correspond to pruned models with high performance across multiple benchmarks.

the Transformer architecture (Vaswani et al., 2017), recent LLMs have shown remarkable scalability and generalization. Over the last few years, the number of released models has grown rapidly (Llama Team, 2024; Qwen Team, 2025; OpenAI, 2025). However, state-of-the-art (SOTA) models often contain billions or even trillions of parameters, making them expensive to train and deploy, which greatly limits their use on resource-constrained devices. Consequently, substantial research effort has focused on compressing LLMs while preserving performance. Importantly, the key question is not only how much knowledge is retained immediately after compression, but how much can be recovered with limited retraining.

Prominent compression strategies include pruning (Sun et al., 2023; Saurav Muralidharan et al., 2024; Guo et al., 2025; Rosenberg et al., 2025), low-rank decomposition (Yuan et al., 2023; Wang et al., 2025; Rausch et al., 2025), quantization (Frantar et al., 2022; Lin et al., 2023), and structural approaches that remove entire transformer blocks (Kim et al., 2024; Song et al., 2024; Men et al., 2025; Gromov et al., 2025; Ding et al., 2025). While weight-level methods are largely orthogonal to each other and can be combined with structural compression, block removal is particularly attractive due to its substantial gains in inference speed and memory efficiency. However, as models

grow deeper and more heterogeneous, block pruning becomes challenging: the effect of removing a given block depends strongly on which other blocks are removed, making it difficult to identify subsets that preserve accuracy at high compression rates.

In this work, we introduce a novel algorithm for selecting combinations of transformer blocks to remove. We associate a binary block-selection variable with each block and construct a second-order approximation of the loss by Taylor-expanding it with respect to these variables and computing an approximate Hessian. This yields a constrained binary optimization (CBO) problem, equivalently expressed as an Ising model with fixed magnetization corresponding to a fixed number of removed blocks.

Although solving this optimization problem is exponentially complex in the number of blocks, it is substantially cheaper than operating on the full model. For the model sizes considered in this work (up to $\mathcal{O}(10^2)$ blocks), the CBO can be solved exactly using brute-force enumeration or classical solvers within minutes to hours on standard CPU hardware. Crucially, we find that not only the minimum-energy solution but also a range of low-energy solutions yield high-quality pruning configurations (see Fig. 1).

Across several benchmarks, these solutions outperform state-of-the-art block-removal methods (Ding et al., 2025; Men et al., 2025; Mistral.AI, 2026) at strong compression rates for Llama-3.1-8B-Instruct (Llama Team, 2024) and Qwen3-14B (Qwen Team, 2025), after short retraining. In particular, we observe significantly improved retention of general knowledge, with MMLU scores (Hendrycks et al., 2020) improving by approximately five to seven percentage points at compression rates exceeding 40%.

We finally show that our method generalizes beyond dense transformers to heterogeneous architectures, including mixture-of-experts models (MoE). Applying our approach to NVIDIA-Nemotron-3-Nano-30B-A3B-FP8 (NVIDIA, 2025), we remove 2 (3) out of 23 MoE blocks, and even without retraining, we retain 94% (91%) and 88% (74%) of the original accuracy on GPQA (Rein et al., 2023) and AIME25, respectively.

While an exact CBO solution becomes infeasible for larger models or more aggressive compression rates, near-optimal solutions are still readily accessible. The fact that the whole low-energy spectrum consistently yields strong pruning configurations ensures that our method remains robust and applicable in more difficult regimes where approximate classical or quantum optimization techniques may be employed (Edward Farhi, 2014; Quinton et al., 2025; Gurobi Optimization, LLC, 2024).

In summary, our main contributions are:

- We formulate transformer block pruning as a CBO by explicitly modeling second-order interactions between blocks, with tractable computational cost for models of practical depth.
- We demonstrate that this formulation outperforms state-of-the-art block-removal techniques on Llama-3.1-8B-Instruct and Qwen3-14B across several benchmarks at high compression rates.
- We show that near-optimal, low-energy solutions provide high-quality pruning configurations, eliminating the need for an exact CBO solution in larger models or aggressive compression regimes.
- We demonstrate that our approach generalizes to heterogeneous mixture-of-experts architectures, yielding strong performance for NVIDIA-Nemotron-3-Nano-30B-A3B-FP8 without retraining.

The remainder of the paper is organized as follows. In Sec. 2, we review related work. In Sec. 3, we introduce our method. We present our results in Sec. 4 and conclude in Sec. 5.

2. Related work

A large body of work has studied the compression of large language models. Existing approaches can broadly be categorized into unstructured and structured pruning methods, low-rank factorization, quantization, and structural approaches that remove entire transformer blocks (often referred to as “depth pruning”). The method presented in this work falls into the last category.

Unstructured and structured pruning methods remove individual weights or entire channels, respectively, and are commonly referred to as width pruning. Representative approaches include magnitude- and sensitivity-based pruning schemes (Sun et al., 2023; Saurav Muralidharan et al., 2024; Guo et al., 2025; Rosenberg et al., 2025). Another widely studied class of methods relies on low-rank factorization of weight matrices, often implemented via SVD-based decompositions or learned low-rank representations, while accounting for calibration data to minimize performance degradation (Yuan et al., 2023; Wang et al., 2025; Rausch et al., 2025). Quantization constitutes a complementary line of work, reducing numerical precision to improve memory footprint and inference efficiency (Frantar et al., 2022; Lin et al., 2023), and can typically be combined with pruning or block-removal methods.

Structural approaches that remove entire transformer blocks aim to directly reduce model depth and inference cost. Prior work in this area includes analyzing how input representations evolve across blocks (Men et al., 2025; Gromov et al., 2025; Mistral.AI, 2026), estimating block importance via

various heuristic or sensitivity-based metrics (Kim et al., 2024; Song et al., 2024), and incorporating block merging strategies (Ding et al., 2025). While effective in certain regimes, these methods generally rely on local or greedy criteria and do not explicitly model interactions between blocks when selecting a global subset to remove.

Our approach is inspired by second-order pruning techniques that rely on a Taylor expansion of the loss function. Such methods were first introduced in the context of weight pruning by Optimal Brain Damage (LeCun et al., 1989) and later extended to combinatorial formulations, such as the Combinatorial Brain Surgeon (Yu et al., 2022), with further scalability improvements via iterative schemes (Rosenberg et al., 2025). However, these works focus on removing individual weights or channels rather than entire transformer blocks.

In contrast, we introduce auxiliary block-selection variables and use a second-order approximation of the loss to explicitly model interactions between blocks. This formulation naturally leads to a constrained binary optimization problem over block configurations, enabling a global, interaction-aware selection of transformer blocks to remove.

3. Method

Our method extends the ideas from the Combinatorial Brain Surgeon (Yu et al., 2022) to block removal. In that work, the authors describe how to identify which weights to prune by solving a combinatorial optimization problem. To adapt this approach to block-level pruning, we introduce a coupling variable α_i for each transformer block i , consisting of an attention block $ATTN$ and a feedforward neural network block FFN . The residual connections in the forward pass are modified as follows:

$$h_{\text{output}} = ATTN(h_{\text{input}}) \cdot \alpha_i + h_{\text{input}}, \quad (1)$$

$$h_{\text{output}} = FFN(h_{\text{input}}) \cdot \alpha_i + h_{\text{input}}. \quad (2)$$

This modification is illustrated in Fig. 2. We initialize $\alpha_i = 1$ for all i , which recovers the original model.

Next, we pass a calibration dataset through the model and consider the change in the cost function $\mathcal{L}(\alpha)$ under perturbations $\delta\alpha = \alpha - \alpha^0$ by performing a Taylor expansion (LeCun et al., 1989; Hassibi et al., 1993; Kurtic et al., 2022; Rosenberg et al., 2025):

$$\begin{aligned} \delta\mathcal{L}(\alpha) &= \mathcal{L}(\alpha) - \mathcal{L}(\alpha^0) \\ &\simeq -\delta\alpha^\top \nabla \mathcal{L}(\alpha^0) + \frac{1}{2} \delta\alpha^\top H^0 \delta\alpha + \mathcal{O}(\delta\alpha^3), \end{aligned} \quad (3)$$

where we define the Hessian matrix $H^0 = \nabla^2 \mathcal{L}(\alpha^0)$. In the following, we assume $\nabla \mathcal{L}(\alpha^0) \approx 0$ for a well-trained model, and neglect the first-order term [as in (LeCun et al.,

1989)], in contrast to (Rosenberg et al., 2025), where including the first-order term was reported to improve results. In all the calculations presented in this work, we use the cross-entropy as the cost function.

Similar to Ref. (Yu et al., 2022), we introduce binary variables x_i , where $x_i = 1$ means that the block is pruned, and write

$$\delta\alpha_i = \alpha_i - \alpha_i^0 = (1 - x_i)\alpha_i^0 - \alpha_i^0 = -x_i\alpha_i^0, \quad (4)$$

meaning that if $x_i = 1$, the block is removed, otherwise it is retained. We are then left with the following constrained binary optimization problem:

$$\begin{aligned} \min_{\mathbf{x} \in \{0,1\}^N} \quad & \mathbf{x}^\top H^0 \mathbf{x} \\ \text{subject to} \quad & \sum_{i=1}^N x_i = M. \end{aligned} \quad (5)$$

Here, M denotes the number of blocks to be removed and N the total number of blocks in the model. We further approximate the Hessian as (Spall, 2005)

$$H^0 \simeq \frac{1}{m} \mathcal{A}^\top \mathcal{A}, \quad (6)$$

where \mathcal{A} is a matrix of per-sample gradients and m is the number of samples.

The number of feasible solutions scales as $\binom{N}{M}$, and the problem can be solved by brute force in many realistic scenarios. We emphasize that the computational complexity depends on both the total number of blocks and the number of blocks removed; consequently, the problem is tractable when either quantity is relatively small. More generally, the problem can be reformulated as a quadratic unconstrained binary optimization (QUBO) problem by introducing a penalty term, which allows it to be solved using highly optimized classical or quantum solvers (Edward Farhi, 2014; Quinton et al., 2025; Gurobi Optimization, LLC, 2024).

Lastly, we emphasize that a key strength of our method is that the Hessian only needs to be computed once, after which Eq. (5) can be solved for a variety of different values of M .

4. Experiments

To evaluate the accuracy of our method, we remove 8 and 16 blocks from Llama-3.1-8B-Instruct (Llama Team, 2024), which has 32 blocks, and 8 and 12 blocks from Qwen3-14B (Qwen Team, 2025), which has 40 blocks. As a calibration dataset for generating the Hessian, we use 2048 samples randomly drawn from OpenHermes-2.5 (Teknium, 2023). After compression, we retrain the models using knowledge distillation (Saurav Muralidharan et al., 2024) for

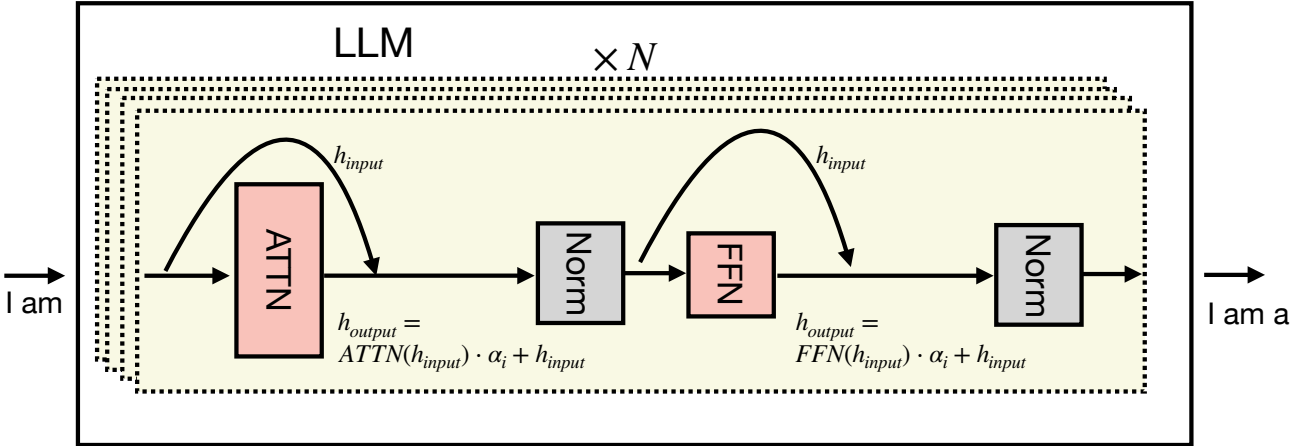


Figure 2. Sketch of the implementation of our algorithm. For each i of the N transformer blocks in the LLM, we introduce an additional parameter α_i that multiplicatively modulates the output of the attention and feedforward blocks.

one/a half (Llama-3.1-8B-Instruct/Qwen3-14B) epoch on OpenHermes-2.5 to mitigate the noise introduced by block removal. The teacher models are loaded with 4-bit quantization using the NF4 scheme (Dettmers et al., 2023), and we use a global batch size of 64 for Llama-3.1-8B-Instruct and 16 for Qwen3-14B. The remaining hyperparameters are provided in our code. All benchmarks are evaluated using the lm-eval-harness (Gao et al., 2024).

4.1. Low-lying excited states

One interesting aspect of our method is that it naturally provides a set of multiple high-quality candidate configurations when compressing an LLM. Once Eq. (5) is set up, it is straightforward to examine both the ground state (lowest-energy eigenvector) and low-lying excited states in cases where solving the optimization problem exactly is feasible. This allows alternative block-removal configurations to be explored without recomputing the Hessian.

For example, for the Llama-3.1-8B-Instruct model, when removing 16 out of the 32 blocks, we find that the ground state suggests removing the blocks [14,16–24,26–31], and that the first 16 low-energy states are quite similar, as they all remove blocks starting from approximately the tenth block onward. However, the 17th excited state, which removes the blocks [2,16,18–31], is the first configuration that proposes removing a block close to the beginning of the model, making it an interesting candidate for further inspection.

In Fig. 3, we show how often each block is selected for removal among the first 20 low-energy states. The results indicate that the algorithm strongly favors removing blocks toward the end of the model, consistent with previous block-pruning approaches (see Appendix A for a list

of block indices removed by different methods). Only a single configuration proposes removing block 2. Notably, after short retraining, this excited-state configuration outperforms the ground state across several benchmarks. This observation disproves the common heuristic assumption that high-quality pruning solutions consist of consecutive blocks (Gromov et al., 2025), and highlights the importance of addressing the full combinatorial nature of the problem.

In Fig. 4, we report accuracy on MMLU (Hendrycks et al., 2020), Winogrande (Sakaguchi et al., 2019), GSM8K (Cobbe et al., 2021), and the BBH leaderboard (Suzgun et al., 2022). We observe that the excited state outperforms the ground state on all tested benchmarks.

Overall, we find that while the ground state typically provides a strong compression baseline, slightly better solutions can often be found among low-lying excited states, depending on the target benchmark. This behavior is a useful feature of our formulation. In scenarios where the optimization problem can be solved exactly, practitioners can inspect several low-energy solutions and select configurations with distinct structural properties, such as removing blocks from different regions of the model. In cases where brute-force optimization is infeasible due to the size of the search space, the problem can instead be reformulated as a QUBO problem and addressed using classical or quantum optimization methods (Edward Farhi, 2014; Quinton et al., 2025; Gurobi Optimization, LLC, 2024). Since our results show that identifying the exact ground state is not always necessary—or even optimal—such approximate solvers are expected to still yield high-quality solutions. Furthermore, algorithms explicitly designed to explore excited states (Altelarrea-Ferré et al., 2025) may provide additional promising alternatives.

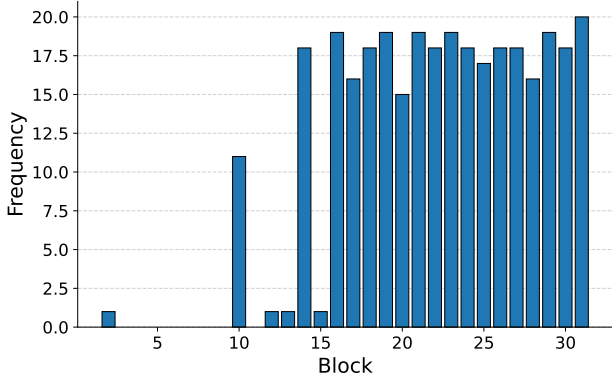


Figure 3. Number of times each block is recommended for removal among the first 20 low-energy states for the Llama-3.1-8B-Instruct model.

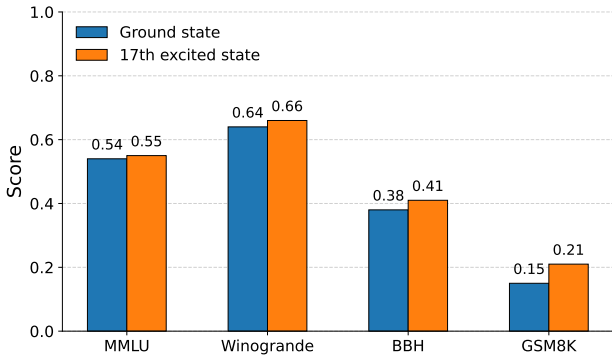


Figure 4. Selected benchmark results for the Llama-3.1-8B-Instruct model with 16 blocks removed. The ground state removes the blocks [14,16–24,26–31] and 17th excited state the blocks [2,16,18–31].

Lastly, we want to note that since some of the energies are close to degenerate, the exact order may be slightly modified in some cases due to numerical rounding errors and should be taken into account when evaluating the models.

4.2. Comparison against SOTA approaches

We now compare CBO against block influence (BI) (Men et al., 2025), sliding window merging (SWM) (Ding et al., 2025), and norm ratio (Mistral.AI, 2026), using the same calibration data and retraining procedure for all methods. Block influence is applied iteratively: one block is removed at a time, and the importance scores are recomputed after each removal. In addition to the benchmarks discussed above, we also evaluate Hellaswag (Zellers et al., 2019) and the ARC Challenge (Clark et al., 2018).

Table 1 summarizes the performance of all methods across benchmarks. In Appendix A, we provide the specific block indices removed by each algorithm.

When removing 8 blocks from Llama-3.1-8B-Instruct, we see very little difference between BI and the CBO ground state (CBO:0). BI scores a bit higher on BBH, while CBO:0 scores a bit higher on GSM8K. Notably, both achieve significantly higher scores for MMLU than SWM and the Norm ratio. When we remove 16 blocks, we observe that the best-performing configuration across all benchmarks except GSM8K corresponds to the 17th excited state (CBO:17). Both the ground state and this excited state significantly outperform BI and SWM on MMLU by 11 and 5 points, respectively, indicating superior retention of general knowledge.

We continue our comparison by removing 8 blocks from Qwen3-14B. There, we see that CBO:0 scores four points higher for MMLU while having three points less for the ARC challenge. Lastly, we remove 12 blocks from Qwen3-14B. There, we see a significantly higher MMLU score compared to the other methods. The remaining benchmarks are very close, except for Hellaswag and the ARC challenge, where BI scores three points higher, and BBH, where CBO:0 scores five points higher.

In general, we want to note that GSM8K results should be interpreted with caution, as we empirically find that these scores are easier to improve through additional fine-tuning (with some care devoted to targeting the output format and reasoning style) than metrics such as MMLU that aggregate many subjects.

Finally, we note that our method is, in principle, compatible with layer-merging approaches. Exploring how these techniques can be effectively combined is left for future work.

4.3. Generalization to Heterogeneous and Mixture-of-Experts Architectures

We next evaluate our method on NVIDIA-Nemotron-3-Nano-30B-A3B-FP8 (NVIDIA, 2025), a hybrid transformer architecture significantly more challenging than standard dense transformers. The model interleaves Mamba2 layers, attention layers, and MoE layers in a non-uniform block structure, making block-removal decisions substantially more complex.

The block layout of the model can be summarized as *MEMEM*EMEMEM*EMEMEM*EMEMEM*EMEMEM*EMEMEM*EMEMEMEM*EMEMEMEM*EMEMEMEMEM*, where *M* denotes a Mamba2 layer, *** an attention layer, and *E* an MoE layer.

In our implementation, we attach the gating parameter α_i to

Table 1. Benchmarks for different block-removal algorithms. # br means number of blocks removed and CBO: # means that we show the # state with 0 corresponding to the lowest energy eigenvalue.

| # br | Model | MMLU | Hellaswag | Winogrande | ARC challenge | BBH | GSM8K |
|------|-------------------------------|-------------|-------------|-------------|---------------|-------------|-------------|
| 0 | Llama-3.1-8B-Instruct | 0.68 | 0.60 | 0.74 | 0.54 | 0.51 | 0.70 |
| 8 | CBO: 0 | 0.64 | 0.53 | 0.71 | 0.45 | 0.45 | 0.66 |
| | BI (Men et al., 2025) | 0.65 | 0.52 | 0.71 | 0.44 | 0.48 | 0.61 |
| | SWM (Ding et al., 2025) | 0.58 | 0.54 | 0.72 | 0.45 | 0.44 | 0.63 |
| | Norm ratio (Mistral.AI, 2026) | 0.45 | 0.51 | 0.63 | 0.38 | 0.36 | 0.34 |
| 16 | CBO: 0 | 0.54 | 0.42 | 0.64 | 0.33 | 0.38 | 0.15 |
| | CBO: 17 | 0.55 | 0.43 | 0.66 | 0.35 | 0.41 | 0.21 |
| | BI (Men et al., 2025) | 0.43 | 0.39 | 0.60 | 0.30 | 0.35 | 0.14 |
| | SWM (Ding et al., 2025) | 0.49 | 0.43 | 0.63 | 0.31 | 0.40 | 0.33 |
| | Norm ratio (Mistral.AI, 2026) | 0.37 | 0.42 | 0.57 | 0.31 | 0.35 | 0.15 |
| 0 | Qwen3-14B | 0.77 | 0.61 | 0.73 | 0.59 | 0.63 | 0.89 |
| 8 | CBO: 0 | 0.71 | 0.51 | 0.70 | 0.47 | 0.52 | 0.78 |
| | BI (Men et al., 2025) | 0.67 | 0.53 | 0.70 | 0.48 | 0.51 | 0.80 |
| | SWM (Ding et al., 2025) | 0.66 | 0.52 | 0.70 | 0.49 | 0.47 | 0.78 |
| | Norm ratio (Mistral.AI, 2026) | 0.54 | 0.53 | 0.69 | 0.50 | 0.43 | 0.77 |
| 12 | CBO: 0 | 0.69 | 0.47 | 0.69 | 0.43 | 0.51 | 0.71 |
| | BI (Men et al., 2025) | 0.62 | 0.50 | 0.69 | 0.46 | 0.46 | 0.72 |
| | SWM (Ding et al., 2025) | 0.61 | 0.48 | 0.69 | 0.45 | 0.45 | 0.70 |
| | Norm ratio (Mistral.AI, 2026) | 0.45 | 0.49 | 0.63 | 0.45 | 0.38 | 0.63 |

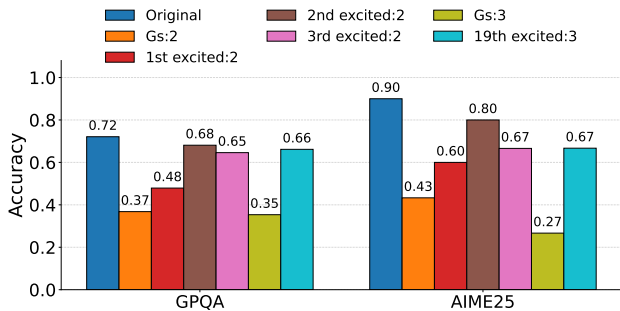


Figure 5. Benchmark results for NVIDIA-Nemotron-3-Nano-30B-A3B-FP8. We use the following notation: Gs:2 means the ground state (lowest-energy eigenvector) of the CBO problem when removing two layers, while, e.g., 19th excited:3 means the 19th excited state when removing 3 layers. See Tab. 2 for the corresponding block index combinations.

each individual block when constructing the Hessian. While alternative formulations could be considered, we leave their exploration for future work. Notably, due to the presence of MoE layers, applying layer-merging approaches such as those proposed in (Ding et al., 2025) becomes non-obvious, further highlighting the difficulty of this setting.

For this experiment, our goal is to test whether any blocks can be removed from such a heterogeneous architecture while maintaining strong downstream performance, without

performing any retraining. To this end, we restrict block removal to MoE layers only, aiming to reduce the on-disk model size while minimally affecting model behavior.

Benchmarks are evaluated on GPQA (Rein et al., 2023) and AIME25 using the Nemo Skills library (NVIDIA NeMo Team, 2025). As calibration data for the Hessian, we use 2048 samples of synthetic data covering code, mathematics, science, chat, and agentic tasks.

Figure 5 shows benchmark results after removing 2 and 3 blocks, corresponding to approximately 8% and 12% parameter reduction. For the model with two blocks less, we show the ground state (Gs:2), which removes blocks [8,10], as well as several low-lying excited states: the first excited state removes blocks [10,36], the second excited state removes blocks [8,45], and the third excited state removes blocks [8,38]. We observe that multiple configurations allow blocks to be removed without a significant degradation in performance. In particular, the configuration corresponding to the second excited state achieves strong accuracy retention across both benchmarks, despite the absence of any retraining. When removing three blocks and looking at the ground state (Gs:3), we see a significant drop in accuracy. However, the 19th excited state (which we identified by analysing good candidates with two blocks removed) still demonstrates the possibility of removing three blocks while maintaining good scores on both benchmarks.

These results demonstrate that our approach generalizes beyond homogeneous dense transformers to complex, hetero-

geneous architectures that include MoE and non-attention-based components. Moreover, they further reinforce the central observation of this work: low-energy excited states can yield high-quality pruning configurations, even in challenging architectural settings.

5. Conclusion

In this work, we introduced a constrained binary optimization (CBO)–based algorithm for selecting which transformer blocks to remove from LLMs. Our approach introduces an auxiliary block-coupling variable for each block and uses a second-order Taylor expansion of the loss to explicitly model interactions between them. This formulation yields a CBO problem whose low-energy solutions correspond to diverse block-removal configurations with high performance across multiple benchmarks. Importantly, we find that the low-energy spectrum contains many high-quality solutions, allowing practitioners to select configurations that best match specific accuracy or structural requirements, rather than relying solely on the global optimum.

We applied our method to Llama-3.1-8B-Instruct and Qwen3-14B and showed that the resulting pruned models outperform those obtained by state-of-the-art block-removal algorithms across a range of benchmarks. Most notably, our models consistently achieve substantially higher MMLU scores, indicating superior retention of general knowledge under strong compression.

We further demonstrated that our approach generalizes beyond homogeneous dense transformers to hybrid architectures with mixture-of-experts (MoE) layers. In particular, for NVIDIA-Nemotron-3-Nano-30B-A3B-FP8, we successfully removed two and three expert layers while maintaining high accuracy on GPQA and AIME25, even without any retraining. This highlights the robustness of our formulation in challenging, non-homogeneous architectural settings.

Efficiently compressing LLMs while preserving their knowledge remains an active and rapidly evolving research area, and several promising extensions of our work remain. For example, instead of manually inspecting low-energy solutions, similarity or diversity scores like the Pearson coefficient could be introduced to automatically select promising candidate configurations. Furthermore, our method is largely orthogonal to existing pruning approaches and could be combined with other compression schemes (Sun et al., 2023; Saurav Muralidharan et al., 2024; Guo et al., 2025; Rosenberg et al., 2025), which we leave for future work.

Acknowledgements

We acknowledge Donostia International Physics Center (DIPC), Ikerbasque, Basque Government, Diputación de

Gipuzkoa, European Innovation Council (EIC), Institute for Advanced Studies in Basic Sciences (IASBS), and Spanish Government for constant support as well as insightful discussions with Sukhbinder Singh, Safa Hamreras, and Alejo Lopez Avila.

Impact Statement

The goal of this work is to advance the development of effective compression algorithms for LLMs. Progress in this area can have a meaningful societal impact by reducing the computational and hardware requirements needed to deploy and fine-tune LLMs, thereby lowering energy consumption and enabling broader access to these technologies. By facilitating more efficient deployment on resource-constrained systems, such methods can contribute to the responsible and more equitable use of LLMs.

References

Altelarrea-Ferré, E., Barberà-Rodríguez, J., Jansen, D., and Acín, A. Beyond ground states: Physics-inspired optimization of excited states of classical Hamiltonians. *arXiv:2507.1239*, 2025. URL <https://doi.org/10.48550/arXiv.2507.1239>.

Clark, P., Cowhey, I., Etzioni, O., Khot, T., Sabharwal, A., Schoenick, C., and Tafjord, O. Think you have solved question answering? try ARC, the AI2 reasoning challenge. *ArXiv*, abs/1803.05457, 2018.

Cobbe, K., Kosaraju, V., Bavarian, M., Hilton, J., Nakano, R., Hesse, C., and Schulman, J. Training verifiers to solve math word problems, 2021.

Dettmers, T., Pagnoni, A., Holtzman, A., and Zettlemoyer, L. QLORA: efficient finetuning of quantized LLMs. In *Proceedings of the 37th International Conference on Neural Information Processing Systems*, NIPS ’23, Red Hook, NY, USA, 2023. Curran Associates Inc.

Ding, X., Sun, R., Zhang, Y., Yan, X., Zhou, Y., Huang, K., Fu, S., Aviles-Rivero, A. I., Xie, C., and Zhu, Y. Sliding-window merging for compacting patch-redundant layers in LLMs. *arXiv:2502.19159*, 2025. URL <https://arxiv.org/abs/2502.19159>.

Edward Farhi, Jeffrey Goldstone, S. G. A quantum approximate optimization algorithm. *arXiv:1411.4028*, 2014. URL <https://arxiv.org/abs/1411.4028>.

Frantar, E., Stock, P., Klett, J., Löwe, T., Brox, T., and Peters, J. GPTQ: Accurate post-training quantization for generative pre-trained transformers. *arXiv preprint arXiv:2210.17323*, 2022.

Gao, L., Tow, J., Abbasi, B., Biderman, S., Black, S., DiPofi, A., Foster, C., Golding, L., Hsu, J., Le Noac'h, A., Li, H., McDonell, K., Muennighoff, N., Ociepa, C., Phang, J., Reynolds, L., Schoelkopf, H., Skowron, A., Sutawika, L., Tang, E., Thite, A., Wang, B., Wang, K., and Zou, A. The language model evaluation harness, 07 2024. URL <https://zenodo.org/records/12608602>.

Gromov, A., Tirumala, K., Shapourian, H., Glorioso, P., and Roberts, D. The unreasonable ineffectiveness of the deeper layers. In *The Thirteenth International Conference on Learning Representations*, 2025. URL <https://openreview.net/forum?id=ngmEcEer8a>.

Guo, J., Chen, X., Tang, Y., and Wang, Y. SlimLLM: Accurate structured pruning for large language models. In *Forty-second International Conference on Machine Learning*, 2025. URL <https://openreview.net/forum?id=2xjUkU7FDb>.

Gurobi Optimization, LLC. Gurobi Optimizer Reference Manual, 2024. URL <https://www.gurobi.com>.

Hassibi, B., Stork, D., and Wolff, G. Optimal brain surgeon: Extensions and performance comparisons. In Cowan, J., Tesauro, G., and Alspector, J. (eds.), *Advances in Neural Information Processing Systems*, volume 6. Morgan-Kaufmann, 1993. URL https://proceedings.neurips.cc/paper_files/paper/1993/file/b056eb1587586b71e2da9acfe4fb19e-Paper.pdf.

Hendrycks, D., Burns, C., Basart, S., Zou, A., Mazeika, M., Song, D., and Steinhardt, J. Measuring massive multitask language understanding. *arXiv:2009.03300*, 2020. URL <https://arxiv.org/abs/2009.03300>.

Kim, B.-K., Kim, G., Kim, T.-H., Castells, T., Choi, S., Shin, J., and Song, H.-K. Shortened LLaMA: A simple depth pruning for large language models. *ICLR Workshop on Mathematical and Empirical Understanding of Foundation Models (ME-FoMo)*, 2024. URL <https://openreview.net/forum?id=18VGxu0dpu>.

Kurtic, E., Campos, D., Nguyen, T., Frantar, E., Kurtz, M., Fineran, B., Goin, M., and Alistarh, D. The optimal BERT surgeon: Scalable and accurate second-order pruning for large language models. In Goldberg, Y., Kozareva, Z., and Zhang, Y. (eds.), *Proceedings of the 2022 Conference on Empirical Methods in Natural Language Processing*, pp. 4163–4181, Abu Dhabi, United Arab Emirates, December 2022. Association for Computational Linguistics. doi: 10.18653/v1/2022.emnlp-main.279. URL <https://aclanthology.org/2022.emnlp-main.279>.

LeCun, Y., Denker, J., and Solla, S. Optimal brain damage. In Touretzky, D. (ed.), *Advances in Neural Information Processing Systems*, volume 2. Morgan-Kaufmann, 1989. URL https://proceedings.neurips.cc/paper_files/paper/1989/file/6c9882bbac1c7093bd25041881277658-Paper.pdf.

Lin, J., Tang, J., Liu, H., Yang, X., Zhang, J., and Han, S. AWQ: Activation-aware weight quantization for llm compression and acceleration. *arXiv preprint arXiv:2306.00978*, 2023.

Llama Team, A. . M. The Llama 3 herd of models. *arXiv:2407.21783*, 2024. URL <https://arxiv.org/abs/2407.21783>.

Men, X., Xu, M., Zhang, Q., Wang, B., Lin, H., Lu, Y., Han, X., and weipeng chen. ShortGPT: Layers in large language models are more redundant than you expect, 2025. URL <https://openreview.net/forum?id=JMNht3SmcG>.

Mistral.AI. Minstral 3. *arXiv:2601.08584*, 2026. URL <https://arxiv.org/abs/2601.08584>.

NVIDIA. Nemotron 3 Nano: Open, efficient mixture-of-experts hybrid Mamba-Transformer model for Agentic reasoning, 2025. URL <https://arxiv.org/abs/2512.20848>. Technical report.

NVIDIA NeMo Team. NeMo-Skills: A collection of pipelines to improve skills of large language models. <https://github.com/NVIDIA-NeMo/Skills>, 2025. GitHub repository, accessed 2026-01-14.

OpenAI. GPT-4 technical report. *arXiv:2303.08774*, 2023. URL <https://arxiv.org/abs/2303.08774>.

OpenAI. gpt-oss-120b & gpt-oss-20b model card, 2025. URL <https://arxiv.org/abs/2508.10925>.

Quinton, F. A., Myhr, P. A. S., Barani, M., Crespo del Granado, P., and Zhang, H. Quantum annealing applications, challenges and limitations for optimisation problems compared to classical solvers. *Scientific Reports*, 15(1):12733, 2025. doi: 10.1038/s41598-025-96220-2. URL <https://doi.org/10.1038/s41598-025-96220-2>.

Qwen Team. Qwen3 technical report, 2025. URL <https://arxiv.org/abs/2505.09388>.

Rausch, R., Jansen, D., Singh, S., and Orús, R. Globally optimized SVD compression of LLMs via fermi-function-based rank selection and gauge fixing. *arXiv:2512.03062*, 2025. URL <https://doi.org/10.48550/arXiv.2512.03062>.

Rein, D., Hou, B. L., Stickland, A. C., Petty, J., Pang, R. Y., Dirani, J., Michael, J., and Bowman, S. R. GPQA: A graduate-level google-proof Q&A benchmark, 2023.

Rosenberg, G., Brubaker, J. K., Schuetz, M. J. A., Zhu, E. Y., Kadioğlu, S., Borujeni, S. E., and Katzgraber, H. G. Scalable iterative pruning of large language and vision models using block coordinate descent. *arXiv:2411.17796*, 2025. URL <https://arxiv.org/abs/2411.17796>.

Sakaguchi, K., Bras, R. L., Bhagavatula, C., and Choi, Y. WinoGrande: An adversarial winograd schema challenge at scale. *arXiv preprint arXiv:1907.10641*, 2019.

Saurav Muralidharan, S., Turuvekere Sreenivas, S., Joshi, R., Chochowski, M., Patwary, M., Shoeybi, M., Catanzaro, B., Kautz, J., and Molchanov, P. Compact language models via pruning and knowledge distillation. *arXiv:2407.14679*, 2024. URL <https://arxiv.org/abs/2407.14679>.

Song, J., Oh, K., Kim, T., Kim, H., Kim, Y., and Kim, J.-J. SLEB: Streamlining LLMs through redundancy verification and elimination of transformer blocks. In *Proceedings of the 41st International Conference on Machine Learning*, 2024.

Spall, J. C. Monte Carlo computation of the Fisher information matrix in nonstandard settings. *Journal of Computational and Graphical Statistics*, 14(4):889–909, 2005. ISSN 10618600. URL <http://www.jstor.org/stable/27594155>.

Sun, M., Liu, Z., Bair, A., and Kolter, J. Z. A simple and effective pruning approach for large language models. *arXiv preprint arXiv:2306.11695*, 2023.

Suzgun, M., Scales, N., Schärli, N., Gehrman, S., Tay, Y., Chung, H. W., Chowdhery, A., Le, Q. V., Chi, E. H., Zhou, D., and Wei, J. Challenging BIG-bench tasks and whether chain-of-thought can solve them. *arXiv preprint arXiv:2210.09261*, 2022.

Teknium. OpenHermes 2.5: An open dataset of synthetic data for generalist llm assistants, 2023. URL <https://huggingface.co/datasets/teknium/OpenHermes-2.5>.

Vaswani, A., Shazeer, N., Parmar, N., Uszkoreit, J., Jones, L., Gomez, A. N., Kaiser, Ł., and Polosukhin, I. Attention is all you need. *Advances in Neural Information Processing Systems*, 30, 2017.

Wang, X., Zheng, Y., Wan, Z., and Zhang, M. SVD-LLM: Truncation-aware singular value decomposition for large language model compression. In *International Conference on Learning Representations (ICLR)*, 2025. URL <https://openreview.net/forum?id=LNYIUouhdt>.

Yu, X., Serra, T., Ramalingam, S., and Zhe, S. The combinatorial brain surgeon: Pruning weights that cancel one another in neural networks. In *Proceedings of the 39th International Conference on Machine Learning*, pp. 25668–25683. PMLR, 2022.

Yuan, Z., Shang, Y., Song, Y., Yang, D., Wu, Q., Yan, Y., and Sun, G. ASVD: Activation-aware singular value decomposition for compressing large language models. *arXiv:2312.05821*, 2023. URL <https://arxiv.org/abs/2312.05821>.

Zellers, R., Holtzman, A., Bisk, Y., Farhadi, A., and Choi, Y. HellaSwag: Can a machine really finish your sentence? In *Proceedings of the 57th Annual Meeting of the Association for Computational Linguistics*, 2019.

Table 2. Blocks removed using the different models.

| # br | Model | Method | Blocks removed |
|------|------------------------|-------------------------------|---|
| 8 | Llama-3.1-8B-Instruct | CBO: 0 | [20,23,25,27,28,29,30,31] |
| 8 | Llama-3.1-8B-Instruct | BI (Men et al., 2025) | [25, 24, 23, 22, 21, 20, 19, 18] |
| 8 | Llama-3.1-8B-Instruct | SWM (Ding et al., 2025) | [[6,7],[12,13],[24-30]] |
| 8 | Llama-3.1-8B-Instruct | Norm ratio (Mistral.AI, 2026) | [8,10,11,12,13,14,19,20] |
| 16 | Llama-3.1-8B-Instruct | CBO: 0 | [14,16,17,18,19,20,21,22,23,24,26,27,28,29,30,31] |
| 16 | Llama-3.1-8B-Instruct | CBO: 17 | [2,16,18,19,20,21,22,23,24,25,26,27,28,29,30,31] |
| 16 | Llama-3.1-8B-Instruct | BI (Men et al., 2025) | [25,24,23,22,21,20,19,18,17,16,15,13,10,9,8,15] |
| 16 | Llama-3.1-8B-Instruct | SWM (Ding et al., 2025) | [[6,7],[8-10],[14-16],[19-30]] |
| 16 | Llama-3.1-8B-Instruct | Norm ratio (Mistral.AI, 2026) | [8,9,10,11,12,13,14,15,19,20,22,23,24,25,27,29] |
| 8 | Qwen3-14B | CBO: 0 | [30,32,33,35,36,37,38,39] |
| 8 | Qwen3-14B | BI (Men et al., 2025) | [35,34,33,32,22,2,2,28] |
| 8 | Qwen3-14B | SWM (Ding et al., 2025) | [[18,19],[23-25],[32-34],[35-38]] |
| 8 | Qwen3-14B | Norm ratio (Mistral.AI, 2026) | [11,12,13,14,15,16,18,39] |
| 12 | Qwen3-14B | CBO: 0 | [2,26,30,31,32,33,34,35,36,37,38,39] |
| 12 | Qwen3-14B | BI (Men et al., 2025) | [35,34,33,32,22,2,2,28,17,17,8,24] |
| 12 | Qwen3-14B | SWM (Ding et al., 2025) | [[14-16],[21,22],[26,27],[24,25],[31-38]] |
| 12 | Qwen3-14B | Norm ratio (Mistral.AI, 2026) | [10,11,12,13,14,15,16,17,18,20,23,39] |
| 2 | NVIDIA-N3N-30B-A3B-FP8 | CBO:0 | [8,10] |
| 2 | NVIDIA-N3N-30B-A3B-FP8 | CBO:1 | [10,36] |
| 2 | NVIDIA-N3N-30B-A3B-FP8 | CBO:2 | [8,45] |
| 2 | NVIDIA-N3N-30B-A3B-FP8 | CBO:3 | [8,38] |
| 3 | NVIDIA-N3N-30B-A3B-FP8 | CBO:0 | [8,10,38] |
| 3 | NVIDIA-N3N-30B-A3B-FP8 | CBO:19 | [8,38,45] |

A. Appendix

In Table 2, we show which blocks were removed by the different methods. For SWM, we show which layers were merged together, whereas for BI, we show the order in which the blocks were removed. Note that for BI, the indices reflect the number of blocks of the current model. This means that if we start with a model with N blocks, [23,22,27] means that we first remove block 23, then recompute the block influence and remove block 22, then recompute the block influence and remove the 27th block (of a model with $N-2$ blocks).